Decreasing Asian summer monsoon intensity after 1860 AD in the global warming epoch

Hai Xu · Yetang Hong · Bin Hong

Abstract The trend of the Indian summer monsoon (ISM) intensity and its nature during the past 100 and 200 years still remain unclear. In this study we reconstructed the ISM intensity during the past 270 years from tree ring $\delta^{18}O$ at Hongyuan, eastern edge of the Tibet Plateau. The monsoon failures inferred from $\delta^{18}O_{\text{tree ring}}$ correlate well with those recorded in ice cores, speleothem, and historical literature sources. 22.6, 59.0, and 110.9-years frequency components in the Hongyuan $\delta^{18}O_{\text{tree ring}}$ series, which may be the responses to solar activities, synchronize well with those recorded in other ISM indices. A notable feature of the reconstructed ISM intensity is the gradually decreasing trend from about 1860 to the present, which is inversely related to the increasing temperature trend contemporaneously. Such "decreasing ISM intensity–increasing temperature" tendency can also be supported by ice core records and meteorological records over a wide geographic extension. The decrease in sea surface temperature gradient between tropical and north Indian Ocean, and the decrease in land-sea thermal contrast between tropical Indian Ocean and "Indian sub-continent–western Himalaya" are possibly responsible for the observed decreasing ISM trend.

Keywords Hongyuan · Tree ring · $\delta^{18}O$ · Indian summer monsoon

H. Xu (✉)
State Key Laboratory of Loess and Quaternary Geology,
Institute of Earth Environment, Chinese Academy of Sciences,
Fenghui South Road, #10, High Tech Zone, Xi'an 710075,
Shaanxi Province, China
e-mail: xuhai2003@263.net

Y. Hong · B. Hong
State Key Laboratory of Environmental Geochemistry, Institute
of Geochemistry, Chinese Academy of Sciences, Guiyang, China

1 Introduction

One of the mostly concerned issues, especially under a global warming scenario, is the future trend of the Indian summer monsoon (ISM) rainfall. Although variations of the ISM on different timescales are well studied, the trend during the past 100 and 200 years is strongly debatable. For instance, most climate model simulations show increasing ISM rainfall trends under a global warming scenario (Meehl and Washington 1993; Douville et al. 2000; May 2002). Sediment records from the Arabian Sea also indicated a significant increasing ISM trend during the past 400 years (Anderson et al. 2002). However, the meteorological ISM rainfall data all over India show no clear long term trend from 1871 to the present. Moreover, increasing evidence shows declined rather than intensified ISM rainfall during the past 100 and 200 years. For example, the meteorological rainfall records of northeastern India, Nepal, and Bangladesh, show a clear decreasing trend during the past century (Duan et al. 2004; Naidu et al. 2009). The past 50 years witnessed an even severe decline of monsoon rainfall over North Africa, e.g. Sahel (Giannini et al. 2003) and parts of monsoonal China (Xiang et al. 2007). It is also notable that the ISM intensity recorded in Dasuopu ice core shows a decreasing trend from about 1850 to the present (Duan et al. 2004; Thompson et al. 2000). Moreover, a speleothem ISM record in Oman (Burns et al. 2002) also shows a general decreasing trend during the past century. Considering these contradicting results, what is the real ISM trend during the past 100 and 200 years, and what is the underlying cause? It is urgent to develop more local and regional ISM records to make clear the trend of ISM during the past 100 and 200 years, and to understand the nature of this trend and how it might continue in the near future.

2 Background and method

During boreal summer, ISM enters into China through the "water vapor channel", southeastern Tibetan plateau, and moves northwards along the eastern edge of the Tibetan plateau (Fig. 1). Tree-ring cores (*Picea likiangensis var. rubescens*) were collected using an increment borer at Shuajingsi town (32°01′N, 102°37′E; Alt.: around 3500 m near the timberlines), Hongyuan County 2004 (Xu et al. 2010). Mean annual temperature at Hongyuan is 1.1 °C, and mean January and July temperature are −10.3 and 10.9 °C, respectively. Mean relative humidity is about 70 ± 3 %. Mean annual precipitation is 700 mm, and about 80 % is centered during June to September.

Cross dating was performed following the skeleton plot method (Stokes & Smiley 1968) and twelve cores without missing and false rings from six trees were selected for stable isotope analysis (Xu et al. 2010). The selected tree-ring cores were sampled with annual resolution and then each year was pooled (Borella et al. 1998), frozen with liquid nitrogen and hammered to powder. For larger rings an attempt was made to visually trim equal masses from each year into the pool, while for narrow rings whole years were pooled together regardless of mass, which may result in trees with narrower rings having less impact on the final $\delta^{18}O$ value of the pooled sample. Alpha cellulose

was prepared using a modified sodium chlorite oxidation method (Hong et al. 2000), including a final NaOH rinse of the samples. Delta ^{13}C of these α-cellulose samples were previously studied, and the results verified the reliability of both the chronology and the pre-treatments (Xu et al. 2010). In this study, we used these α-cellulose samples to measure oxygen isotopes on a mass spectrometer (Finnigan Mat-252), with experimental precision better than ±0.2 ‰. We measured each sample more than twice, and got an average $\delta^{18}O$ value for each calendar year. Experiments were performed in 2007 at the State Key Laboratory of Environmental Geochemistry, Institute of Geochemistry, Chinese Academy of Sciences. The last 50 samples (sample 1–50; covering 1955–2004) were repeatedly measured 2009 at the same laboratory to verify the reproducibility.

Another two cores, core SJS-17 and SJS-12, also without missing and false rings, but with very narrow ring widths for some sections, were cut off every five rings. Delta ^{18}O series of these two individual cores were established in 2009 using the same method to verify the robustness of chronology and data measurements. SJS-17 series covers 1600–1898, with two missing points due to the insufficiency of samples; while SJS-12 covers 1895–2001. As shown in Fig. 2, the Hongyuan $\delta^{18}O_{\text{tree ring}}$ series highly synchronize with $\delta^{18}O$ series of the other two

Fig. 1 Sampling sites. *Red star* denotes the tree-ring sampling site at Shuajingsi town (SJS), while *yellow dashed curve* and *filled green stars* indicate the transect and the carex sampling sites. *Yellow circles* denote the locations of Hongyuan (HY), Songpan (SP), Guangyuan (GY), Chengdu (CD), and Yushu (YS). Also shown are locations of Dasuopu (DSP) and Rongbuk (RBK) ice cores (*filled blue triangles*). *Arrow-lines* in upper panel show the streamlines averaged from June to August at 850 hPa during 1968–1996 based on the NCEP/NCAR reanalysis data (Kalnay et al. 1996). *Gray arrow* in lower panel sketchily shows the "vapor channel" at the southeast Tibet plateau
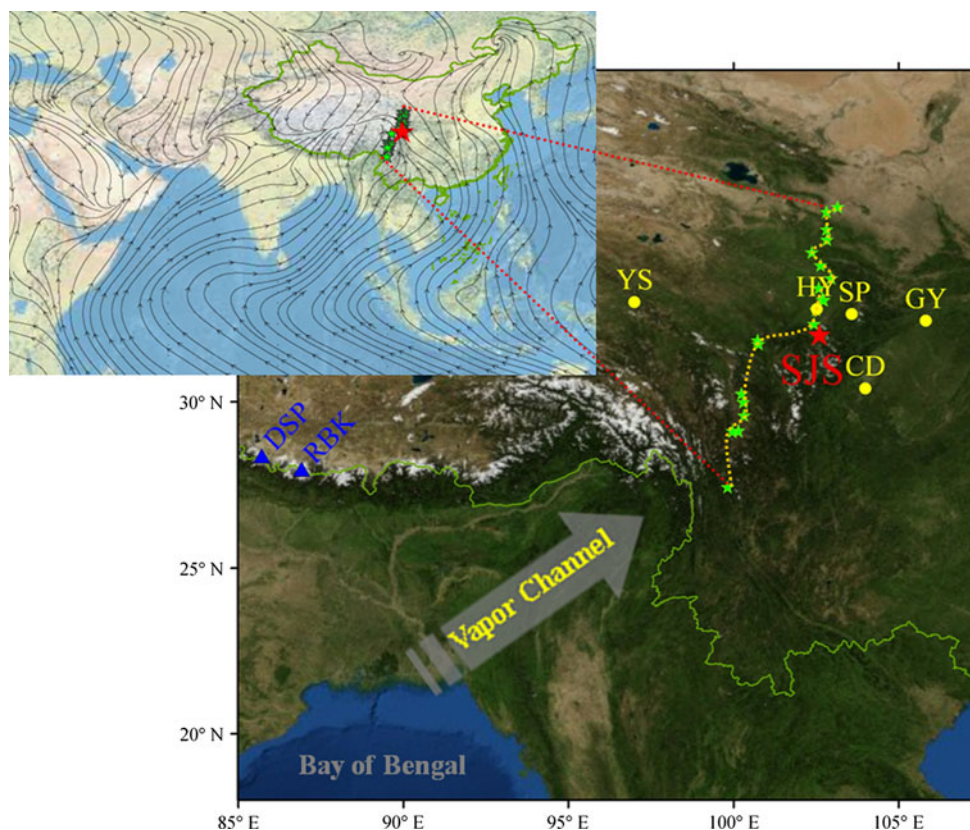
Fig. 2 Hongyuan tree ring δ^{18}O timeseries. *Gray* and *pink* curves represent the Hongyuan δ^{18}O$_{tree\ ring}$ series and the duplicates of the last 50 years, respectively. The *blue curve* denotes five year running mean of Hongyuan δ^{18}O$_{tree\ ring}$ series. *Green curve* with *blank circles* and *orange curve* with *filled triangles* represent δ^{18}O series of SJS-17 and SJS-12 samples (see text), respectively
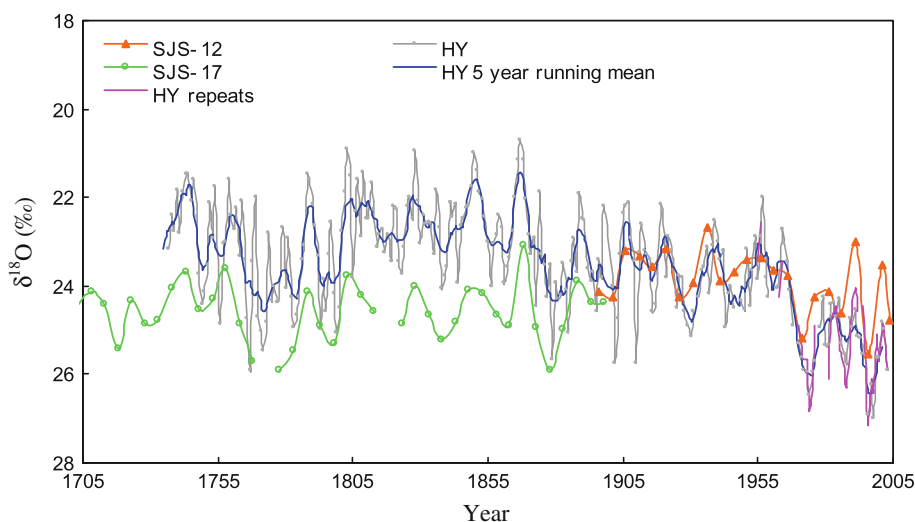
individual cores, supporting both the reliability of chronology and the reproducibility of δ^{18}O measurements.

In 2007, we also selectively collected living sedges (*Carex* sp.) growing without groundwater supply along the easten edge of the Tibet plateau (Fig. 1) and measured δ^{18}O$_{carex}$, 2009, using a similar method than for the tree ring samples. The purpose was to understand the "δ^{18}O$_{rainfall}$–climatic factor" relationship from the "δ^{18}O$_{carex}$–climatic factor" relationship, assuming δ^{18}O$_{carex}$ and δ^{18}O$_{rainfall}$ have similar spatial variations (see below).

3 Climatic significance of Hongyuan δ^{18}O$_{tree\ ring}$

As already demonstrated by Dansgaard (1964), temperature is generally the dominating factor controlling δ^{18}O$_{rainfall}$ at high latitudes (examples can be seen in Greenland and Antarctica ice cores); while precipitation amounts significantly influence δ^{18}O$_{rainfall}$ at low latitudes. At middle to middle-low latitudes, δ^{18}O$_{rainfall}$ is generally influenced both by temperature and precipitation. From an oxygen isotopic fractionation perspective, if the oxygen isotopic fractionation is dominated by temperature, then δ^{18}O$_{rainfall}$ is expected to be positively correlated to temperature ($\delta = aT + b$, where $a > 0$). On the other hand, if δ^{18}O is dominated by the precipitation amount effect, then δ^{18}O$_{rainfall}$ should be negatively correlated to precipitation (Dansgaard 1964). Observation data show that monthly δ^{18}O$_{rainfall}$ at Chengdu area is negatively correlated to precipitation ($r = -0.53$, $\alpha = 0.11$; Fig. 3a). In summer, δ^{18}O$_{rainfall}$ is low and precipitation is high; while in winter, δ^{18}O$_{rainfall}$ is high but precipitation is low (Fig. 3a). This suggests that δ^{18}O$_{rainfall}$ is dominated by the amount effect around the study area, and therefore is linked to monsoon precipitation. The δ^{18}O variations in speleothem

carbonates in southern China have also been suggested to be controlled by precipitation, and are widely used as indicators of monsoon intensity (Yuan et al. 2004; Wang et al. 2005; Zhang et al. 2008). Weak ISM is related to low precipitation and high δ^{18}O$_{rainfall}$ values; while strong ISM corresponds with high precipitation and low δ^{18}O$_{rainfall}$ values.

For plants that directly use rainfall water as source water, the δ^{18}O in plant cellulose is largely enriched compared with δ^{18}O$_{rainfall}$. This enrichment, called as biological fractionation, is relatively constant (about 27‰), and therefore the variability of δ^{18}O$_{plant}$ is mainly derived from that of δ^{18}O$_{rainfall}$ (Roden et al. 2000; Miller et al. 2006; Xu et al. 2006). As shown in Fig. 3c, the spatial variation of δ^{18}O$_{carex}$ is negatively correlated to precipitation. Since *Carex* we selectively collected has short roots and uses rainfall water directly as source water, the δ^{18}O$_{carex}$ variability can be used as a substitute of δ^{18}O$_{rainfall}$ variability. Therefore, a negative spatial correlation pattern of "δ^{18}O$_{rainfall}$–precipitation" can be inferred from that of "δ^{18}O$_{carex}$–precipitation", providing independent evidence that the rainfall δ^{18}O around the study site is dominated by precipitation, and thus ISM intensity.

As shown in Fig. 3d, the Hongyuan δ^{18}O$_{tree\ ring}$ is significantly correlated to relative humidity. Since relative humidity and precipitation show similar annual variations (Fig. 3b) and monthly distribution patterns (correlation coefficient is 0.932, $\alpha < 0.001$; figure not shown), the Hongyuan δ^{18}O$_{tree\ ring}$ can be related to monsoon precipitation, and thus ISM intensity. Higher δ^{18}O$_{tree\ ring}$ relates to weaker ISM intensity, and vice versa. Such "δ^{18}O$_{tree\ ring}$–monsoon intensity" relationship is also consistent with that found by Sano et al. (2010) in the Nepal Himalaya and that found by Grießinger et al. (2011) in the southern Tibetan plateau most recently.

Fig. 3 **a** Monthly rainfall $\delta^{18}O$ and precipitation at Chengdu (see location in Fig. 1), **b** averaged May to September relative humidity and precipitation of Hongyuan during 1958–2003. **c** scatter plots between *Carex* $\delta^{18}O$ and precipitation along the eastern edge of the Tibetan Plateau (Fig. 1). d. scatter plots between tree ring $\delta^{18}O$ and relative humidity (five years running mean)
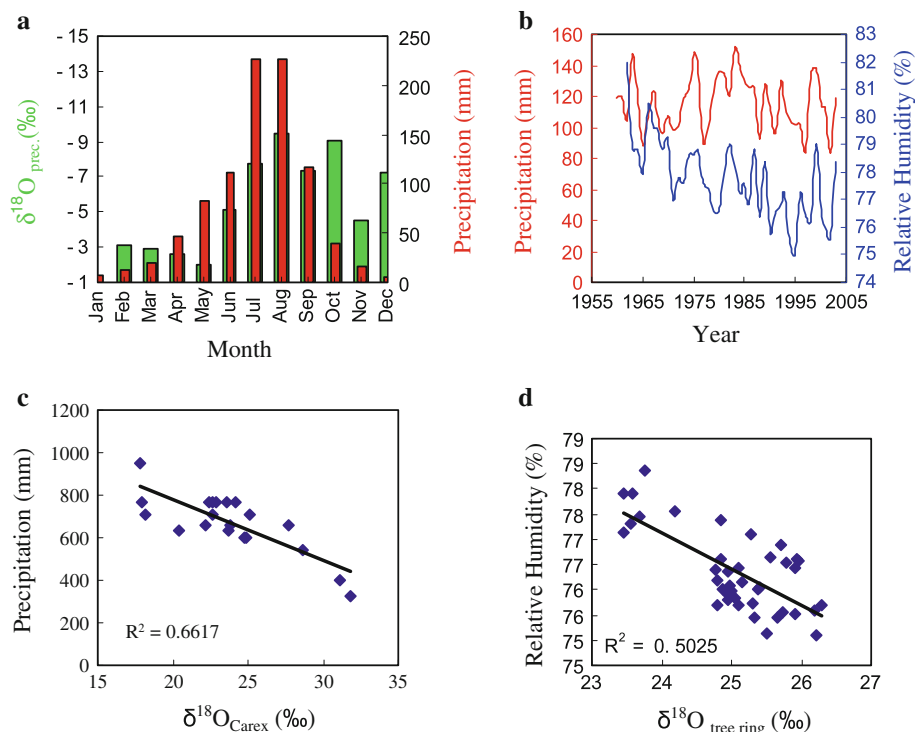
4 Comparison of $\delta^{18}O_{tree\ ring}$ with other precipitation records

One of the direct rainfall archives are ice cores. The accumulation rate of Rongbuk ice core, which is closely related to the northeastern Indian summer precipitation, recorded the variation of ISM intensity during the past about 160 years (Zhang et al. 2004). As shown in Fig. 4, the Hongyuan $\delta^{18}O_{tree\ ring}$ curve shows high correlation with the Rongbuk accumulation rate curve ($r = -0.39$; $\alpha < 0.001$), supporting the use of $\delta^{18}O_{tree\ ring}$ as an indicator of monsoon precipitation. Thompson et al. (2000) suggested that the dust content in Dasuopu ice core is a sensitive indicator of ISM intensity. As shown in Fig. 4 (see shaded columns), most of the climatic events recorded in Dasuopu ice core also correlate well with those inferred from Hongyuan $\delta^{18}O_{tree\ ring}$, especially from 1860 to the present. The Chinese Drought/Flood (D/F) indices, which were derived from historical literature records (Zhang et al. 2003), have been widely used as precipitation proxy indices. As shown in Fig. 4, the climatic events recorded in $\delta^{18}O_{tree\ ring}$ are generally consistent with those recorded in the D/F index of Guangyuan. Similar climatic events can also be found in the Oman speleothem record regardless of some small age difference during the past 300 years (Burns et al. 2002).

The ISM inferred from $\delta^{18}O_{tree\ ring}$ dropped dramatically during 1760–1800, and reached the lowest values at about 1788–1795, which is very similar with that recorded in

speleothem (Burns et al. 2002). At about 1867, ISM decreased again, and was minimum about 1879, consistent with the widely reported "1877 Indian big famine" (Pant and Rupa Kumar 1997). Such a clear monsoon failure can also be seen in ice core records and the Drought/Flood indices. At about 1895–1902, a strong ISM reduction can be detected in the $\delta^{18}O_{tree\ ring}$ curve, similar to those recorded in Rongbuk and Dasuopu ice cores, Guangyuan D/F index, and Oman S3 (Fig. 4). Around 1927 and 1942 are another two obvious ISM reductions, which are also clear in Rongbuk and Dasuopu ice cores and in the D/F index series. The $\delta^{18}O_{tree\ ring}$ and D/F indices show significant drops from the middle 1960s, reaching the twentieth century minimum at the middle 1970s, in accordance with the Rongbuk snow accumulation curve (Fig. 4). This strong monsoon drop can also be detected from meteorological records over a wide geographical extension, from North Africa (e.g. Sahel) to northern India, to southwest China, and even to north China (Yan et al. 1990).

One striking feature of the $\delta^{18}O_{tree\ ring}$ curve is that from 1700 to about 1860, the $\delta^{18}O_{tree\ ring}$ shows no clear long term trend, while an obviously decreasing trend can be seen from about 1860 to the present (Fig. 4). The dust content in Dasuopu ice core shows a similar long term behavior with $\delta^{18}O_{tree\ ring}$, i.e. generally stable from 1700 to 1860, and decreasing from about 1860 to the present. The accumulation rate at Dasuopu, which is highly correlated with the northeastern Indian precipitation (Duan et al. 2004), also shows a significant decrease after about 1850.

Fig. 4 Comparison between precipitation indices of Hongyuan $\delta^{18}O_{tree\ ring}$, Rongbuk ice accumulation (Zhang et al. 2004), Dasuopu dust concentration (Thompson et al. 2000), Drought/Flood index of Guangyuan (5-years running mean) (Zhang et al. 2003), and $\delta^{18}O$ of Oman speleothem S3 (Burns et al. 2002). *Shaded columns* indicate ISM failures and *dotted lines* indicate the long-term rainfall trend. All *curves* (except the Drought/Flood index) are annually scaled with five-point running means
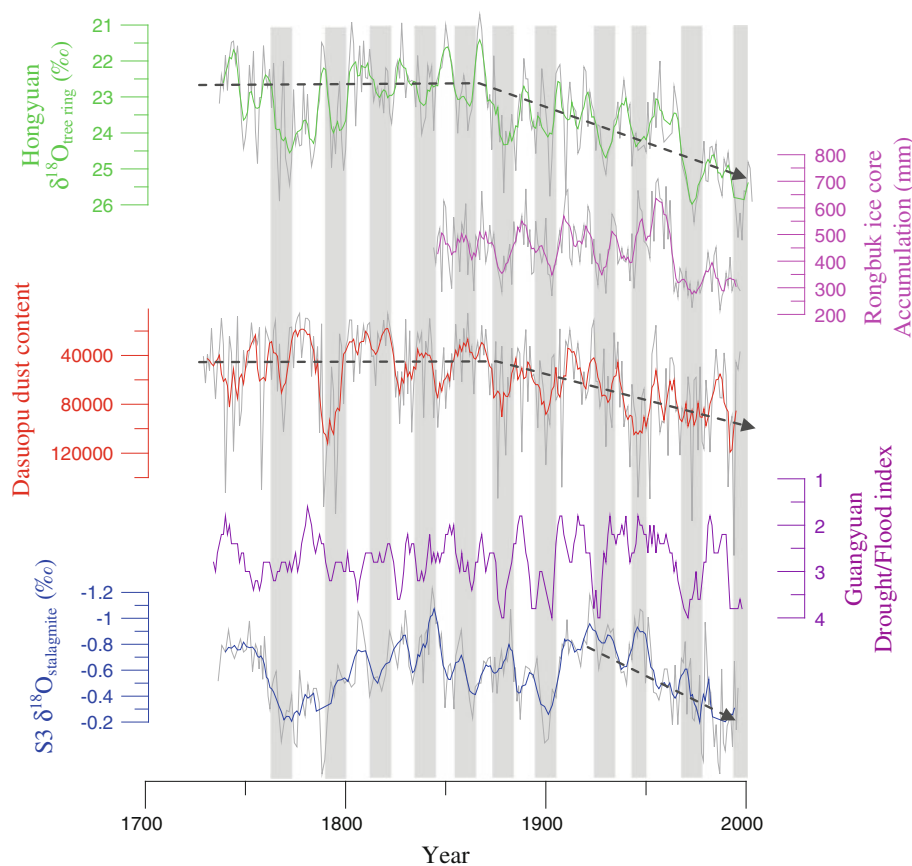
Such decreasing trends can also be found in southern Oman speleothem records during the past century (Fig. 4) (Burns et al. 2002). Meteorological rainfall records from northeastern India (Naidu et al. 2009), Nepal, and Bangladesh (Duan et al. 2004) also show decreasing trends during the past 100 years. Summer precipitation inferred from tree ring $\delta^{18}O$ in southern Tibet also indicates a decreasing monsoon precipitation trend during the past 100 and 200 years (Grießinger et al. 2011). These evidences illustrate that the ISM intensity during the past 100 and 200 years is gradually decreasing rather than increasing.

5 Discussion

5.1 Periodicities in $\delta^{18}O_{tree\ ring}$ series

On short term timescales, more and more evidence shows strong linkages between annual variations in ISM and the El Niño Southern Oscillation (ENSO) (Kumar et al. 2006). The interannual rainfall in Sahel region is also obviously influenced by ENSO (while its low frequency variability is closely linked to SSTs of the tropical Ocean; see below) (Giannini et al. 2003). We previously found an inverse relationship between temperature at the study site and

$SST_{Niño3}$ (an indicator of El Niño events) on multi-annual scale, which is attributed to the potential heating of ISM rainfall associated with ENSO (Xu et al. 2010). However, the annual variations in $\delta^{18}O_{tree\ ring}$ do not show significant correlation with $SST_{Niño3}$. The power spectrum analysis also failed to detect significant high frequency components in the $\delta^{18}O_{tree\ ring}$ series. This is possibly due to the influences of some local processes on source water $\delta^{18}O$ on short term timescale, e.g. evaporation and hydrological mixture between surface water and soil water, which masks the high ISM frequency.

It is interesting to show by Fast Fourier Transform (FFT) analysis that there exist three significant periodicities in $\delta^{18}O_{tree\ ring}$ series, namely 110.9, 59.0, and 22.6-years (Fig. 5). A significant 22 year cycle can also be obtained from the FFT analysis of the Rongbuk ice accumulation series (calculated from Zhang et al. 2004). Hiremath and Mandi (2004) found a 22-years cycle in ISM rainfall. Duan et al. (2004) found a 25-years cycle in the Dasuopu ice accumulation series. These similar cycles suggest a common quasi-22-years cycle in the ISM variability, which is possibly a response to the 22-years variation of solar activity. FFT analysis shows a significant 25-years cycle in the Yushu (see location in Fig. 1) temperature series reconstructed from tree ring widths (Liang et al. 2008). The

Fig. 5 a Periodicities (**a** and **b**) in Hongyuan $\delta^{18}O_{tree\ ring}$ series (examined by Fast Fourier Transform method on the software of Autosignal). *Green*, *red*, and *blue curves* denote 111, 59.0, and 22.6-years cycles respectively. **c**, **d**, **e** show the comparison between 22.6-years component of Hongyuan $\delta^{18}O_{tree\ ring}$ and 25-years components of Yushu temperature reconstructed from tree ring width (Liang et al. 2008), that between 59.0-years component of Hongyuan $\delta^{18}O_{tree\ ring}$ and the 21-years running mean of June–Sept Indian summer monsoon rainfall (Parthasarathy et al. 1995), and that between 111-years component of Hongyuan $\delta^{18}O_{tree\ ring}$ and $\delta^{18}O$ of S3 (Burns et al. 2002). See text for details
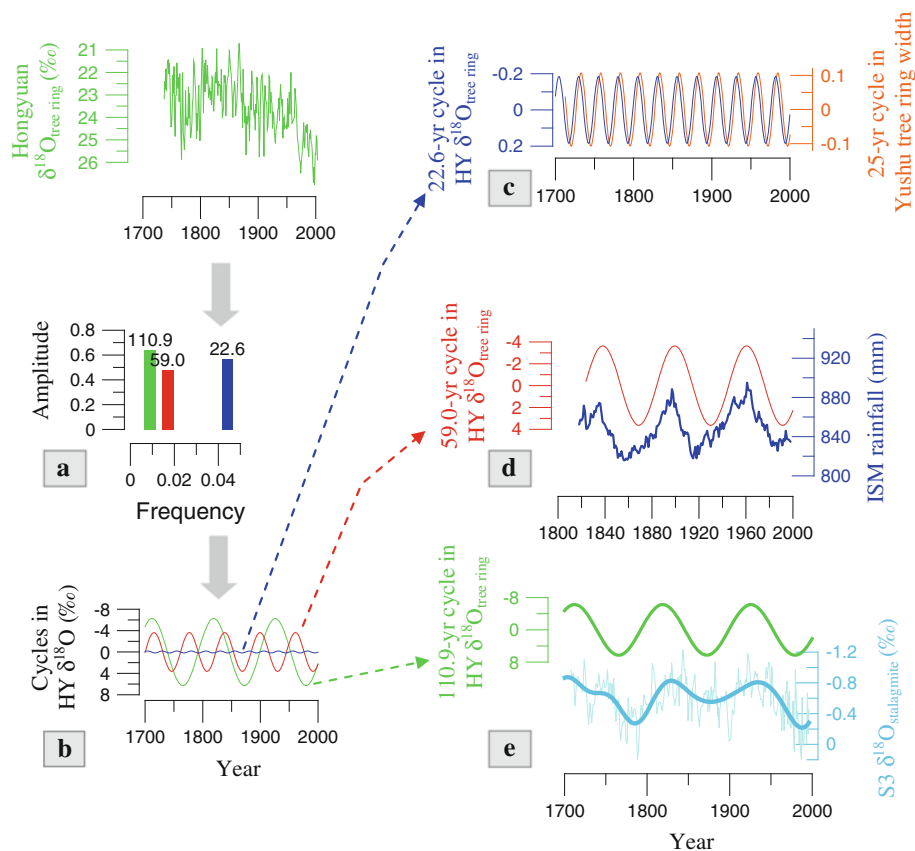
coherence on 22-years cycle between our $\delta^{18}O_{tree\ ring}$ series and the Yushu temperatures (Fig. 5) further validates the application of $\delta^{18}O_{tree\ ring}$ as an indicator of precipitation. An interpretation of the $\delta^{18}O_{tree\ ring}$ as an indicator of temperature would result in an anti-phase relationship between temperature variations at Hongyuan and Yushu, which contradicts the high in-phase relationship as indicated by the meteorological records (figure not shown).

The significant 110.9-years cycles in $\delta^{18}O_{tree\ ring}$ series is a quasi-100-years cycle, which has also been detected in Hongyuan peat records near the study site (Xu et al. 2006). This 110.9-years component shows very similar trend with the ISM record from Oman (Burns et al. 2002) (Fig. 5), supporting strongly that the low frequency climate at Hongyuan area is dominated by ISM. This typical period in ISM variations is also detected in speleothem records of Dongge cave (Wang et al. 2005), and in sediment records from the Arabian Sea (Anderson et al. 2002; von Rad 1999; Agnihotri et al. 2002), suggesting that the quasi-100-years cycle is a common periodicity in the ISM regions.

The 59.0-years cycle is also clear in $\delta^{18}O_{tree\ ring}$ series and is similar in pattern with the quasi-60-years cycle in ISM rainfall record (Fig. 5) (Parthasarathy et al. 1995; Agnihotri and Dutta 2003). Similar periodicities can also be found in the Dongge cave speleothem record (Dykoski,

et al. 2005), and in the cross spectrum between $\delta^{18}O_{stalagmite}$ and atmospheric ^{14}C concentration in both Dongge cave (Wang et al. 2005) and Hoti cave (Neff et al. 2001). A 62-years cycle can also be detected in the FFT spectrum of the Rongbuk ice accumulation series (calculated from Zhang et al. 2004). The ISM proxy indices in northeastern Arabian Sea also show similar periodicities (von Rad 1999; Agnihotri et al. 2002).

A lot of the studies show coherence between solar activity and ISM on centennial to decadal timescales. For example, Wang et al. (2005) showed that the decadal to centennial scale Asian summer monsoon intensity synchronizes with solar activity. Neff et al. (2001) suggested that "one of the primary controls on centennial- to decadal-scale changes in tropical rainfall and monsoon intensity during this time are variations in solar radiation". Agnihotri et al. (2002) showed that on decadal and centennial scale the ISM shows similar variations with solar activity (Periodicities of 200, 105 and 60 yr are observed in the proxy records coinciding with those known for solar cycles). Fleitmann et al. (2003) suggested "decadal to multidecadal variations in monsoon precipitation being linked to solar activity". The 22.6, 59.0, and 110.9-years periodicities extracted from Hongyuan $\delta^{18}O_{tree\ ring}$ series seem to be linked to solar activity.

5.2 Possible mechanism of the decreasing ISM trend

As shown in Fig. 6, the decreasing trend of ISM inferred from our $\delta^{18}O_{tree\ ring}$ series is inversely correlated with the increasing trend of total solar irradiance (Lean 2000) during the past 100 and 200 years. Duan et al. (2000) also found a negative correlation between the long term trend of Dasuopu ice accumulation and solar activity. This suggests that solar activity is at least not the direct forcing for the decreasing ISM trend from 1860 to the present. An increasing temperature trend at the study site (inferred from $\delta^{13}C_{tree\ ring}$, Xu et al. 2010) has been reported most recently, consistent with the observed global warming (Fig. 6). The meteorological records around the study site also show increases in temperature but slight decreases in precipitation. For example, the mean annual temperature increased by about 0.95 centigrade during the past 50 years, while the mean annual precipitation decreased by about 40 mm at Hongyuan during the same interval. Why does the ISM intensity decrease in opposition to an increasing temperature trend? What is the nature of the long term decreasing ISM trend during the past 100 and 200 years?

The north or south movement of Intertropical Convergence Zone (ITCZ) has been widely suggested to be related to Asian summer monsoon intensity (Wang et al. 2005; Fleitmann et al. 2007). In general, higher solar insolation leads to northward movement of ITCZ, and intensified Asian summer monsoon on long term time scale, e.g. millennium timescale. However, for short term timescales, the movement of ITCZ is still not well documented. Recently, Sachs et al. (2009) suggested that the ITCZ zone
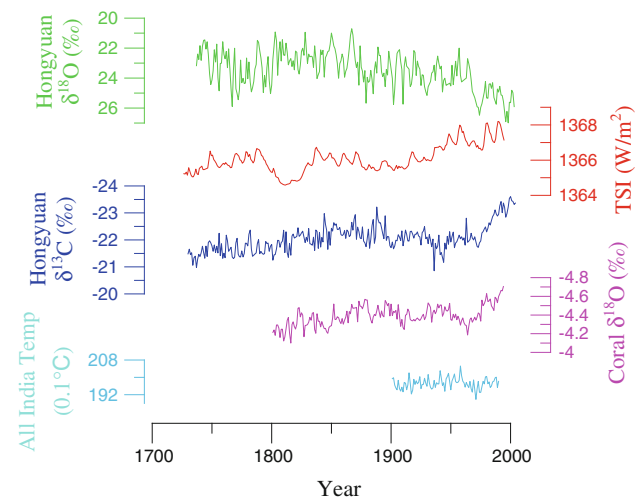
Fig. 6 Comparison between Hongyuan $\delta^{18}O_{tree\ ring}$ (*green*; precipitation proxy index; see text for details), total solar irradiance (TSI, *red*) (Lean 2000), Hongyuan $\delta^{13}C$ (*blue*; temperature proxy index) (Xu et al. 2010), Indian Ocean coral $\delta^{18}O$ (*pink*; temperature proxy index; see Cole et al. (2000) for details), and all Indian temperature records (1901–1990; *sky blue*) (Pant and Rupa Kumar 1997)

shifted southwards significantly during 1400–1850 AD (the Little Ice Age), which implies a northward return after 1850 AD. Thus, if the ISM trend from 1860 to the present is also dominated by ITCZ, then an increasing, rather than decreasing ISM trend can be expected, which is contrary with the observed decline trend.

Numerous studies link the reduced ISM rainfall with changes in SST of the Indian Ocean (e.g. Giannini et al. 2003; Naidu, et al. 2009; Chung and Ramanathan 2006). Accompanied with the global warming, SSTs increase significantly. For example, various sources of SST data reveal that the tropical Indian Ocean, particularly the equatorial portion, has warmed substantially since the 1950s (see Chung and Ramanathan 2006 and references therein). Coral $\delta^{18}O$ records indicate that the sea surface temperature increased both at Malindi and Seychelles (tropical West Indian Ocean) during the past two centuries (Cole et al. 2000). Wilson et al. (2006) showed that SST increased significantly between 30°N and 30°S in Pacific and Indian Oceans from about 1860 to the present. The Hongyuan precipitation (inferred from $\delta^{18}O_{tree\ ring}$) is highly negatively correlated with the Indian Ocean SST (inferred from coral $\delta^{18}O$; $r = -0.44$, $\alpha < 0.001$; Fig. 6; Cole et al. 2000), suggesting a possible linkage between increasing tropical ocean SST and decreasing ISM trend. Giannini et al. (2003) also linked the Sahel drought during the past two decades to the increased SST over the tropical oceans.

It is interesting to note that the SST increase over the equatorial Indian Ocean during the past 50 years is much higher than that over the northern Indian Ocean (Chung and Ramanathan 2006), which leads to an obvious decrease in summertime SST gradient. Ramanathan et al. (2005) ascribed this decreased SST gradient to the green house gases and the aerosol; the former leads to a uniform warming of the tropical Indian Ocean, while the latter has a cooling effect and masks the green house gas warming effect in the northern Indian Ocean. "From a dynamical consideration, a weakening of the SST gradients in the north Indian Ocean can weaken the monsoon circulation, by weakening both the cross-equatorial (south to north) surface pressure gradient and north-to-south mid- and upper troposphere pressure gradient" (Chung and Ramanathan 2006). Therefore, decreasing rather than increasing monsoon circulation can be expected. Naidu et al. (2009) also associated the decreased ISM rainfall with the decreased meridional SST gradient under a global warming era.

The decreased ISM is also possibly related to the decrease in land-sea thermal contrast under an abnormal global warming scenario. Although temperature over the northern hemisphere has been widely reported to increase during the past 100 and 200 years, the increment over land regions where the Indian low pressure develops may be smaller compared with that over sea surface. This is

possibly because the increasing atmospheric brown cloud over the Indian sub-continent and northern Indian Ocean weakened the increase in temperature (Ramanathan et al. 2005). For example, SST at western Indian Ocean increased significantly during the past 100 years inferred from Cole et al. (2000), yet the increase in surface temperature over the Indian sub-continent is rather slight from 1900 to 2000 (Fig. 6). Temperature at Pune, western India, even shows a decreasing trend during the past one hundred years (Gadgil and Dhorde 2005). Except for the aerosol cooling effect, we speculate that the Himalayan snow cover, which has been strongly shrinked during the past decades (e.g. Zhao and Moore 2006), may have dampened the increase in temperature, especially under an abnormal global warming scenario. For example, the spring temperature variations reconstructed from tree ring chronologies over the western Himalaya during the past four centuries showed no clear long term trend, but even indicated "a long-term cooling trend since the late 17th century to early 20th" (Yadav and Singh 2002). The observed data also indicated no clear (or slightly decreasing) long term temperature trend over northwestern India and western Himalaya during the past century (Yadav et al. 2004; Ganguly and Iyer 2009). Meehl and Washington (1993) also showed that the SST of the Indian Ocean increased by 0.28 °C but the south Asian land temperature increased only 0.07 °C from 1971 to 1990. Therefore, a decreased long term land-sea thermal contrast between the equatorial Indian Ocean and Indian sub-continent to western Himalaya under an abnormal global warming scenario can be expected. This decreased land-sea thermal contrast may have led to the decreased summer monsoon rainfall over a wide geographic region during the past three decades, like in the Sahel zone (Giannini et al. 2003), India, Nepal, Bangladesh (Naidu et al. 2009; Chung and Ramanathan 2006), and the southwest to north China (Xiang et al. 2007).

The increased SST leads to more atmospheric moisture transported northward to the summer monsoon regions due to intensified evaporation, which is expected to provide more precipitable water over the ISM region. The decreased monsoon circulation may have counterbalanced the increased atmospheric moisture, and leads to no clear long term rainfall trend over the west and central Indian sub-continent. However, for northeastern India, and for regions along the monsoon flow direction (like areas along the above mentioned "vapor channel" to southwest China), the weakened monsoon flow will eventually lead to decline in monsoon rainfall since much vapor has been precipitated before reaching this area. Therefore, if the global warming continues, the SST over tropical Indian Ocean will persist increasing, while temperature over the north Indian Ocean, the Indian sub-continent, and western Himalaya would keep relatively steady, which will lead to continuous

decreases in SST gradient over the Indian Ocean and decreases in land-sea thermal contrast, and eventually lead to continuously weakening of ISM intensity.

6 Summary

We reconstructed the ISM intensity during the past 270 years from tree ring δ^{18}O at Hongyuan, eastern edge of the Tibet Plateau. The monsoon failures inferred from $\delta^{18}O_{tree\ ring}$ synchronize well with those recorded in other ISM indices. Significant periodicities of 22.6, 59.0, and 110.9-years were detected in the Hongyuan $\delta^{18}O_{tree\ ring}$ series, which may be the responses to solar activities. A notable feature of the reconstructed ISM intensity is the gradually decreasing trend from about 1860 to the present, which is inversely related to the increasing temperature trend contemporaneously. Such "decreasing ISM intensity–increasing temperature" tendency has been suggested to be related to the decrease in sea surface temperature gradient between tropical and north Indian Ocean, and the decrease in land-sea thermal contrast between tropical Indian Ocean and "Indian sub-continent–western Himalaya". Under this circumstance, the ISM intensity would be expected to continue decreasing if the global warming continues.

References

Agnihotri R, Dutta K (2003) Centennial scale variations in monsoonal rainfall (Indian, east equatorial and Chinese monsoons): manifestations of solar variability. Curr Sci 85:459–463

Agnihotri R, Dutta K, Bhushan R, Somayajulu BLK (2002) Evidence for solar forcing on the Indian Monsoon during the last millennium. Earth Planet Sci Lett 198:521–527

Anderson DM, Overpeck JT, Gupta AK (2002) Increase in the Asian southwest monsoon during the past four centuries. Science 297:596–599

Borella S, Leuenberger M, Saurer M, Siegwolf R (1998) Reducing uncertainties in δ^{13}C analysis of tree rings: pooling, milling, and cellulose extraction. J Geophys Res 103(D16):19519–19526. doi:10.1029/98JD01169

Burns SJ, Fleitmann D, Mudelsee M, Neff U, Matter A, Mangini A(2002)A 780-year annually resolved record of Indian Ocean monsoon precipitation from a speleothem from south Oman. J Geophys Res. doi:10.1029/2001JD001281

Chung CE, Ramanathan V (2006) Weakening of North Indian SST gradients and the monsoon rainfall in India and the Sahel. J Clim 19:2036–2045

Cole JE, Dunbar RB, McClanahan TR, Muthiga NA (2000) Tropical Pacific forcing of decadal SST variability in the Western Indian Ocean over the past two centuries. Science 287:617–619

Dansgaard W (1964) Stable isotopes in precipitation. Tellus 16:436–468

Douville H, Royer J-F, Polcher J, Cox P, Gedney N, Stephenson DB, Valdes PJ (2000) Impact of CO_2 doubling on the Asian summer monsoon: robust versus model dependent responses. J Meteor Soc Jpn 78:421–439

Duan KQ, Wang NL, Li YF, Sun WZ (2000) Accumulation in Dasuopu ice core in Qinghai-Tibet plateau and solar activity. Chinese Sci Bull 45:1038–1042

Duan KQ, Yao TD, Thompson LG (2004) Low-frequency of southern Asian monsoon variability using a 295-year record from the Dasuopu ice core in the central Himalayas. Geophys Res Lett. doi:10.1029/2004GL020015

Dykoski CA, Edwards RL, Cheng H, Yuan D, Cai Y, Zhang M, Lin Y, Qing J, An Z, Revenaugh J (2005) A high-resolution, absolute-dated Holocene and deglacial Asian monsoon record from Dongge Cave, China. Earth Planet Sci Lett 233:71–86

Fleitmann D, Burns SJ, Mudelsee M, Neff U, Kramers J, Mangini A, Matter A (2003) Holocene forcing of the Indian Monsoon recorded in a stalagmite from Southern Oman. Science 300:1737–1739

Fleitmann D, Burns SJ, Mangini A, Mudelsee M, Kramers J, Villa I, Neff U, Al-Subbary AA, Buettner A, Hippler D, Matter A (2007) Holocene ITCZ and Indian monsoon dynamics recorded in stalagmites from Oman and Yemen (Socotra). Quat Sci Rev 26:170–188

Gadgil A, Dhorde A (2005) Temperature trends in twentieth century at Pune, India. Atmos Environ 39:6550–6556

Ganguly ND, Iyer KN (2009) Long-tern variations of surface air temperature during summer in India. Int J Climatol 29:735–746

Giannini A, Saravanan R, Chang P (2003) Oceanic forcing of Sahel rainfall on interannual to interdecadal time scales. Science 302:1027–1030

Grießinger J, Bräuning A, Helle G, Thomas A, Schleser G (2011) Late holocene Asian summer monsoon variability reflected by $\delta^{18}O$ in tree-rings from Tibetan junipers. Geophys Res Let 38(L03701):1–5. doi:10.1029/2010GL045988

Hiremath KM, Mandi PI (2004) Influence of the solar activity on the Indian Monsoon rainfall. New Astron 9:651–662

Hong YT, Jiang HB, Liu TS, Zhou LP, Beer J, Li HD, Leng XT, Hong B, Qin XG (2000) Response of climate to solar forcing recorded in a 6000-year $\delta^{18}O$ time-series of Chinese peat cellulose. Holocene 10(1):1–7

Kalnay E et al (1996) The NCEP/NCAR 40-year reanalysis project. Bull Am Meteorol Soc 77:437–470

Kumar KK, Rajagopalan B, Hoerling M, Bates G, Cane M (2006) Unraveling the mystery of Indian monsoon failure during El Niño. Science 314:115–119

Lean J (2000) Evolution of the sun's spectral irradiance since the maunder minimum. Geophys Res Lett 27:2425–2428

Liang EY, Shao XM, Qin NS (2008) Tree-ring based summer temperature reconstruction for the source region of the Yangtze River on the Tibetan Plateau. Glob Planet Change 61:313–320

May W (2002) Simulated changes of the Indian summer monsoon under enhanced greenhouse gas conditions in a global timeslice experiment. Geophys Res Lett. doi:10.1029/2001GL013808

Meehl GA, Washington WM (1993) South Asian summer monsoon variability in a model with doubled atmospheric carbon dioxide concentration. Science 260:1101–1104

Miller DL, Mora CI, Grissino-Mayer HD, Mock CJ, Uhle ME, Sharp Z (2006) Tree-ring isotope records of tropical cyclone activity. Proc Natl Acad Sci USA 103:14294–14297

Naidu CV, Durgalakshmi K, Krishna KM, Rao SR, Satyanarayana GC, Lakshminarayana P, Rao LM(2009)Is summer monsoon rainfall decreasing over India in the global warming era? J Geophys Res. doi:10.1029/2008JD011288

Neff U, Burns SJ, Mangini A, Mudelsee M, Fleitmann D, Matter A (2001) Strong coherence between solar variability and themonsoon in Oman between 9 and 6 kyr ago. Nature 411:290–293

Pant GB, Rupa Kumar K (1997) Climates of South Asia. Wiley, Chichester

Parthasarathy B, Munot AA, Kothawale DR (1995) Contributions from Indian Institute of Tropical Meteorology. Research Report RR-065, Pune. Data from IRI Climate Data Library. http://ingrid.ldeo.columbia.edu/SOURCES/Indices/india/rainfall

Ramanathan V, Chung C, Kim D, Bettge T, Buja L, Kiehl JT, Washington WM, Fu Q, Sikka DR, Wild M (2005) Atmospheric brown clouds: impacts on South Asian climate and hydrological cycle. Proc Natl Acad Sci USA 102:5326–5333

Roden JS, Lin G, Ehleringer JR (2000) A mechanistic model for the interpretation of hydrogen and oxygen isotope ratios in tree ring cellulose. Cosmochim Acta 64:21–35

Sachs JP, Sachse D, Smittenberg RH, Zhang Z, Battisti DS, Golubic S (2009) Southward movement of the Pacific intertropical convergence zone AD 1400–1850. Nat Geosci 2:519–525

Sano M, Sheshshayee MS, Managave S, Ramesh R, Sukumar R, Sweda T (2010) Climatic potential of $\delta^{18}O$ of Abies spectabilis from the Nepal Himalaya. Dendrochronologia 28:93–98

Stokes MA, Smiley TL (1968) An introduction to tree-ring dating. University of Arizona Press, Tucson. (Reprinted 1995), pp xi–xiii, xv–xvii, 3–20

Thompson LG, Yao T, Mosley-Thompson E, Davis ME, Henderson KA, Lin PN (2000) A high-resolution millennial record of the South Asian monsoon from Himalayan ice cores. Science 289:1916–1919

von Rad U (1999) A 5000-yr record of climate change in varved sediments from the oxygen minimum zone off Pakistan, northern Arabian Sea. Quat Res 51:39–53

Wang Y, Cheng H, Kong X, Edwards RL, An Z, Wu J, Dykoski CA, He Y, Kelly MJ, Li X (2005) The holocene Asian Monsoon: links to solar changes and north. Science 308:854–857

Wilson R, Tudhope A, Brohan P, Briffa K, Osborn T, Tett S (2006) Two-hundred-fifty years of reconstructed and modeled tropical temperatures. J Geophys Res. doi:10.1029/2005JC003188

Xiang LY, Chen X, Li CH, Zheng JH (2007) The regional features of abrupt precipitation change in China in recent 55 years. Torre Rain Disasters 26:149–153 (in Chinese with English Abstract)

Xu H, Hong YT, Lin QH, Zhu YX, Hong B, Jiang HB (2006) Temperature responses to quasi-100-yr solar variability during the past 6000 years based on $\delta^{18}O$ of peat cellulose in Hongyuan, eastern Qinghai-Tibet plateau, China. Palaeogeogr Palaeoclimatol Palaeoecol 230:155–164

Xu H, Hong YT, Hong B, Zhu YX, Wang Y (2010) Influence of ENSO on multi annual temperature variations at Hongyuan, NE Qinghai-Tibet plateau: evidence from $\delta^{13}C$ of spruce tree rings. Int J Clim 30:120–126

Yadav RR, Singh J (2002) Tree-ring-based spring temperature patterns over the past four centuries in Western Himalaya. Q Res 57:299–305

Yadav RR, Park WK, Singh J, Dubey B (2004) Do the western Himalayas defy global warming? Geophys Res Lett. doi:10.1029/2004GL020201

Yan Z, Ji J, Ye D (1990) Northern hemispheric summer climatic jump in the 1960s, part I—rainfall and temperature. Sci China Ser B 33:1092–1101

Yuan D, Cheng H, Edwards RL, Dykoski CA, Kelly MJ, Zhang M, Qing J, Lin Y, Wang Y, Wu J, Dorale JA, An Z, Cai Y (2004) Timing, duration, and transitions of the last interglacial Asian monsoon. Science 304:575–578

Zhang DE, Li XQ, Liang YY (2003) Complement of the Chinese drought/flood index during 1993–2000. J Appl Meteorol Sci 14:379–383 (in Chinese)

Zhang DQ, Qin DH, Hou SG, Kang SC, Ren JW (2004) Net accumulation rate of the east Rongbuk Glacier and Indian summer monsoon rainfall. J Glaciol Geocry 2:129–134 (in Chinese with English abstract)

Zhang P, Cheng H, Edwards RL, Chen F, Wang Y, Yang X, Liu J, Tan M, Wang X, Liu J, An C, Dai Z, Zhou J, Zhang D, Jia J, Jin L, Johnson KR (2008) A test of climate, sun, and culture relationships from an 1810-year Chinese cave record. Science 322:940–942

Zhao H, Moore GWK (2006) Reduction in Himalayan snow accumulation and weakening of the trade winds over the Pacific since the 1840s. Geophys Res Lett 33:L17709. doi: 10.1029/2006GL027339